

Improving Generalization of Transfer Learning Across Domains Using Spatio-Temporal Features in Autonomous Driving

Shivam Akhauri², Laura Y. Zheng¹, Tom Goldstein¹, and Ming C. Lin^{1,2}

<https://gamma.umd.edu/stltransfer>

Abstract—Training vision-based autonomous driving in the real world can be inefficient and impractical. Vehicle simulation can be used to learn in the virtual world, and the acquired skills can be transferred to handle real-world scenarios more effectively. Between virtual and real visual domains, common features such as relative distance to road edges and other vehicles over time are consistent. These visual elements are intuitively crucial for human decision making during driving. We hypothesize that these spatio-temporal factors can also be used in transfer learning to improve generalization across domains. First, we propose a CNN+LSTM transfer learning framework to extract the spatio-temporal features representing vehicle dynamics from scenes. Next, we conduct an ablation study to quantitatively estimate the significance of various features in the decisions of driving systems. We observe that physically interpretable factors are highly correlated with network decisions, while representational differences between scenes are not. Finally, based on the results of our ablation study, we propose a transfer learning pipeline that uses saliency maps and physical features extracted from a source model to enhance the performance of a target model. Training of our network is initialized with the learned weights from CNN and LSTM latent features (capturing the intrinsic physics of the moving vehicle w.r.t. its surroundings) transferred from one domain to another. Our experiments show that this proposed transfer learning framework better generalizes across unseen domains compared to a baseline CNN model on a binary classification learning task.

I. INTRODUCTION

Vision-based autonomous driving systems often leverage transfer learning to infer learned skills from source domains (e.g. simulation) to target domains (e.g. real-world scenes). Driving data is often pulled from many domains, both simulated and real. Depending on the quality of a simulator, the changing scenes in a physical location, or other lighting and visibility effects in the captured environment, there can be major visual differences between domains. Despite these representation differences across domains, the underlying structure of environments remains the same; the movement of a vehicle and its interaction with the environment will be similar. For example, an ego camera will collect data containing clear lane markings, axes of rotation, and flow of traffic, regardless of whether the domain is simulated or real. These dynamics, capturing intrinsic physics of moving systems, remain consistent from domain to domain. In this article, we consider transfer learning methods that carry temporal components (e.g. linear and rotational velocity of a

vehicle and acceleration of the vehicle, its motion relative to other dynamic obstacles, etc.), in addition to spatial information (e.g. geometry, size, and configuration of nearby moving agents and the environment), across domains.

We start by considering a range of physical properties of scenes, and we perform an ablation study to measure the importance of each factor for self-driving systems. We consider five natural spatio-temporal visual elements and analyze their contribution in decision making for driving tasks: 1) projected distance to other vehicles, 2) rotation of the vehicle over time, 3) optical flow, 4) color gradients, and 5) moving objects. The first three elements characterize the state of a dynamical system (e.g. vehicle itself) over time, while the last two describe the geometry of the surrounding environment and dynamic obstacles (e.g. other cars, nearby pedestrians and/or animals).

After studying the role of these factors in driving, we consider transfer learning schemes that move spatio-temporal features between domains. We propose to improve transfer learning through a CNN+LSTM architecture, which would support consideration of spatio-temporal features in image sequences during transfer learning. Our transfer learning is conducted in two phases. Phase 1 involves straightforward training of a CNN+LSTM model on a source domain (e.g. simulation image data from one environment in the CARLA simulator [1]). LSTM hidden state embeddings (i.e. parameters/weights of the LSTM) from phase one are transferred to phase 2, which involves training on data from the target domain (possibly from another scene generated by a simulator or a different real-world environment). The phase 2 network trains using target domain image data, in addition to a range of physical features extracted from phase 2 videos using the pre-trained phase 1 model. Phase 2 training data is combined with saliency maps, gradients from the source model, and edge maps. The saliency maps are obtained from preliminary training on phase 2 data in the target domain with learned weights from phase 1 in the source domain. Transfer of spatio-temporal information is done not only through the transfer of network weights and LSTM hidden states, but also through saliency maps extracted from target domain data. Our model shows significant improvements in testing accuracy of up to **37.29%** for unseen environments compared to CNN-only models [2]. Unseen test domains include other simulation data with visual differences and real-world data, which are never introduced to the model during phase one training.

In summary, the main contributions of this work include:

The authors are with ¹Department of Computer Science and ²Maryland Robotics Center, University of Maryland at College Park, MD, U.S.A. E-mail: {sakhauri,lyzheng,tomg,lin}@umd.edu

- 1) A CNN+LSTM model architecture, which extends CNN-only autonomous driving networks [3], to capture both spatial and temporal information;
- 2) Transfer of LSTM hidden state embeddings, in addition to learned weights from the CNN [2], to further facilitate transfer of both spatial and temporal features;
- 3) Dynamics-aware spatio-temporal feature extraction to complement regular image data with saliency, gradient, and edge maps for training in transfer learning.

II. RELATED WORK

A. Attention-based LSTMs

Long short-term memory (LSTM) architectures excel at extracting sequential features. Thus, they are widely used in learning tasks that require historical actions to be considered in predicting the future. Attention mechanisms first employed in natural language processing research can be used to complement the LSTM models in other learning tasks in order to reach better performance. Bahdanau et al. [4] was the first to employ the concept of an encoder-decoder with additive attention in English to French translation. Ba et al. [5] train a reinforcement learning model for a multiple-object recognition task, where the attention mechanism allows the model to recognize the most significant regions of an image. [6] and [7] reached state of the art results by combining LSTM frameworks with attention mechanisms in human action prediction and recognition. Bai et al. [8] present a framework for deep learning based motion planning for autonomous vehicles. This work shows that a CNN and LSTM combined network architecture is able to extract spatio-temporal features from time series autonomous driving data. We seek to extend this work for the purposes of exploring the effect of spatio-temporal features on the decision making process in certain autonomous driving learning tasks.

B. Domain Adaptation in Autonomous Driving

Since autonomous driving is an application that relies heavily on simulated data, domain adaptation is a well-studied topic. In autonomous driving, the purpose of developing domain adaptation methods is to be able to generalize findings in the virtual domain to the physical environment, in practical real-world application of autonomous driving. Several works focus on domain adaptation for segmentation tasks. Zhang et al. introduce a curriculum-style learning approach in order to improve domain adaptation baselines [9]. Domain adaptation work is heavily explored through the use of GANs. Hong et al. incorporated a GAN into their FCN framework, which allows for structured domain adaptation [10]. Outside of autonomous driving specifically, Murez et al. introduced a method for image to image translation for segmentation tasks [11]. This is achieved by finding a latent space where representations in each domain remain agnostic, and features extracted by the backbone encoder network are regularized. While this method is optimized for segmentation tasks, we are inspired by this notion that representations of features in images are agnostic in latent spaces. In autonomous driving, features essential to the

learner’s decision making are often explored by gaze models. In this sense, unseen environments are better generalized due to the emphasis on critical features during learning, instead of more arbitrary background information. One work uses gaze models to improve autonomous driving predicting human gaze with conditional GANs [12]. Aside from this other works, such as SAGE [13] by Pal et al., provides driving specific contextual information in addition to raw human gaze data to improve generalization to unseen environments. In our work, we draw inspiration from both topics of domain adaptation and gaze for contextual information to create a framework that generalizes over unseen environments using critical information in simulated autonomous driving data.

C. Transfer Learning in Autonomous Driving

Transfer learning can be useful in autonomous driving in transferring information learned in one environment to another, or even in one domain to another. Weiss et al. formally define transfer learning as well as current state of the art [14]. [15] applies transfer learning in wilderness traversal, where a lack of real-world wilderness prevents learning from real world data directly. Since the same problem affects autonomous driving in cases such as accident data, transfer learning can be beneficial in transferring learned variables to the real world. Virtual-to-real transfer learning can also be used for reinforcement learning in autonomous driving, as shown by [16]. Likewise, transfer learning has also been shown to improve performance in steering tasks using imitation learning, as shown by [2], which is a transfer learning enhanced framework based on the end-to-end learning model by Bojarski et al. [3]. In our framework, we use a transfer learning framework to transfer learned information on critical decision making components across environments, which allows for better generalization across domains.

D. Similarity Metrics

Image similarity can be quantified in several ways. Chen and Chu review five main ways: Euclidean distance, Mahalanobis Distance, Chord Distance, Pearson’s Correlation Coefficient, and Spearman Rank Coefficient [17]. Image similarity was used here in the practical application of database similarity matching based on color, shape, or texture information. Image similarity metrics can also be used to measure the quality of an image. Horé and Ziou analyze a comparison between peak-signal-to-noise ratio (PSNR) and structural similarity index measure (SSIM) which measures the extent of image degradations such as Gaussian blur, additive Gaussian white noise, jpeg and jpeg2000 compression [18]. Other than image similarity metrics, are text similarity metrics such as cosine similarity of TF-IDF representations. Text similarity metrics must not only measure the direct frequency of words, but also capture semantic and latent information, which is inferred from context and not always directly obvious. Albitar et al. develop a TF-IDF based similarity metric that aggregates semantic similarities between concepts in text documents [19]. TF-IDF vectors in text similarity can be drawn in parallel to hidden state

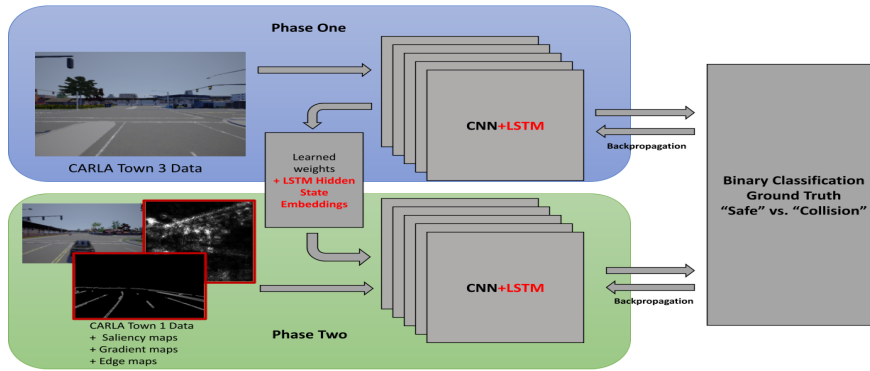


Fig. 1. **Transfer learning training framework.** Phase one, highlighted in blue, represents standard training of the CNN+LSTM network with CARLA Town 3 data. Learned weights from CNN and LSTM hidden state embeddings are transferred to Phase Two, highlighted in green. Phase Two training data from CARLA Town 1 is also complemented with Town 1 saliency, gradient, and edge maps generated from preliminary training of Phase Two. Contributions to traditional CNN-based transfer learning frameworks are highlighted in red.

representations of images in learning models. Our choice is inspired by this work in that we quantify similarity of data contextually on decision-making for autonomous driving.

III. ENHANCED TRANSFER LEARNING

Transfer learning can be useful to vision-based autonomous driving, since data can be sourced from multiple domains, whether virtual simulator or real-world. However, with image data, transfer of useful driving information may be limited by the pixel-level details. These details may include minute differences in quality, coloring, brightness, and other visual differences between virtual and real data.

A. Hypothesis

Conventional transfer learning for vision-based driving generally focuses on spatial features, without considering temporal relations between images. We hypothesize that **generalization of transfer learning can be enhanced by leveraging spatio-temporal features in cross-domain training.** Table III in Appendix shows results where the *resulting trained parameters from the neural network incorporate around 78% of the global spatio-temporal features.*

Key Insights. Our two main contributions towards current transfer learning frameworks are (1) the transfer of spatio-temporal information from both the network model and the image sequences, as opposed to solely spatial information ; and (2) dynamics-aware feature transfer by complementing training data with saliency, gradient, and edge maps. We describe our enhanced transfer learning method in two phases: the first of which represents base training in the source domain and the latter representing training with transferred features from Phase One, along with the extracted spatio-temporal features in saliency maps in Phase Two.

B. Our Transfer Learning Framework

In contrast to the standard CNN-architecture commonly used in self-driving vehicle simulators, we propose to adopt a CNN+LSTM model to improve the generalization of transfer learning across domains, by better exploiting the spatio-temporal features at both the network level and the image training sequences, as shown in Fig. 1.

Model Architecture. Our model architecture consists of two convolutional layers, two inception model components, two LSTM layers, three fully connected layers, and a softmax layer. During training in the source domain, we initialize the hidden states of the LSTM with random noise, as well as initialize the other weights with standard Xavier initialization.

Phase 1 Training. Phase 1 training represents a standard from-scratch training of the network described above. The learning task is the binary classification task of recognizing dangerous from safe scenarios in data. We train this network on data collected from the CARLA simulator [1], e.g. Town 3, as shown in the upper box of Fig. 1.

Phase 2 Training. In phase two, model weights from the CNN and LSTM networks are transferred from the fully-trained phase one network to the phase two network. The phase two dataset is from the target domain, such as a different environment in the CARLA simulator [1], Town 1, or other real-world driving data. Saliency, gradient, and edge maps extracted from phase 2 training data are used to complement this image sequence data for phase 2 training. The transfer of weights represents information transferred between networks through model parameters, while the various generated maps represent spatio-temporal feature transfer through data.

Saliency Maps. Saliency maps process images by differentiating a loss with respect to image pixels. A sequence of saliency maps for a scenario signifies the flow of spatial features *across frames*. These spatio-temporal features are captured as the change in intensities of the pixels on continuous sets of phase 2 data using the model weights from phase 1. The resulting saliency maps are used to complement the original phase 2 dataset during training.

IV. SELECTION OF VISUAL ELEMENTS IN DRIVING

The dynamics and geometry of visual elements should remain constant across virtual and real domains. The vehicle will still follow the same constructs of driving behavior: staying between road markings, turning and rotating around a vertical axes, etc. We study the significance of key visual

elements by observing the change in model parameters over image sequences, measured with cosine similarity.

Studied Elements. We study five different elements to empirically determine their contribution to decision making in driving. These five components are listed below.

- 1) **Projected distance:** the distance (in meters) from nearby vehicles, studied in Table I.
- 2) **Vehicle rotation:** the rotation at which a vehicle is performing at any given moment.
- 3) **Optical flow:** motion flow of objects/pixels in a scene.
- 4) **Gradient information:** change in pixel values, analogous to edge detection, studied in Table II.
- 5) **Moving Objects:** dynamic obstacles in the scene.

While the first three of these capture the states of a dynamical system, the last two characterize the geometry of the surrounding environment and other objects in the scene. Projected distance, vehicle rotation, and dynamic obstacles can be tangibly observed, while optical flow and gradient information are elements that are inferred by the model during learning.

A. Comparison of Image Similarity Metrics

We use the cosine similarity to measure the closeness in image feature representations during the learning process, and compare its ability to correlate to collision confidence with Frchet Inception Distance (FID) and Structural Similarity Index Measure (SSIM).

Frchet Inception Distance [20] measures the distance between two datasets by comparing the mean and standard deviation of the activations in an Inception network. We calculate the FID using [21] in our observations. While FID is powerful and standard for measuring the quality of images synthesized by generative adversarial networks (GANs), it is typically used to measure the distance between two image distributions. In our use case, we are interested in measuring the distance between model parameters upon input images of same (similar) distribution at different points in time. Thus, FID measurements would not be appropriate.

Another metric we consider is the SSIM [22], a perception-based metric primarily used for assessing image quality. SSIM is robust to various transformations and is commonly used in image quality assessments; but it considers pixel-level representations of images, and not semantic representations in learning. This is a stark difference from FID, which is farther from pixel-level representation and closer to learned perception.

Since the focus of our study is to measure the impact of visual components on learning, we require a metric that can also consider the features of the network closer to learned perception, similarly to FID, but on a pairwise basis, where images may be from the same distribution, like the SSIM. We propose using cosine distance between vectors of LSTM hidden layer features x and y formulated as:

$$similarity(x, y) = \frac{x \cdot y}{\|x\| \|y\|}$$

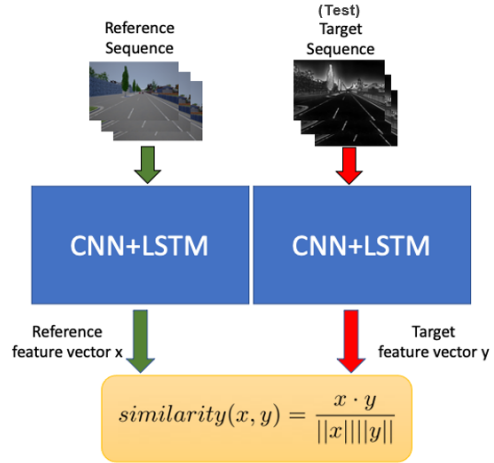


Fig. 2. Method for computing cosine similarity measurements in the ablation study. Reference sequences include base driving images, while target (test) sequences include saliency, gradient, and edge maps. Cosine similarity is computed from feature vectors extracted from intermediary layers of the CNN+LSTM network. Greater similarity measurements (closer to 1) indicate closeness in model perception of the data.

x and y are 32-dimensional vectors that represent hidden state features (i.e. model parameters or weights) extracted from the CNN+LSTM network, for both image sequences. An advantage of cosine similarity over other metrics for comparing vectors, such as Euclidean distance, is that cosine similarity normalizes the magnitude of the vector, not letting the magnitude of the vector or the dimensionality of the data affect the similarity measurement. We show quantitative comparison among the three metrics in Tables I and II.

B. Measurement Methodology

We choose image sequences in which each of the five visual elements named are observed over time. For example, a sequence featuring a change in projected distance may include a vehicle moving closer or farther from the camera. Model representations of the images are obtained from inference of the fully trained network following phase two of transfer learning. We measure four levels of changes in metrics for projected distance, with level 1 being the smallest change in projected distance over time and level 4 being the largest change. Since the learning task is binary classification of “safe” versus “collision”, we expect there to be greater change in measured cosine similarity as collision confidence (i.e. the probability of predicted collision by the model) changes. Intuitively, as nearby vehicles become closer past a certain threshold, the collision confidence will greatly increase. See comparison for projected distance in Table I.

In addition, we observe the differences in learning perception of the base dataset and its gradient and saliency maps, which are measured similarly to projected distance above. We sample three different image sequences for GradCAM [23] and Vanilla Gradient [24], where collision confidence is equal. We do this to measure the difference in model-level perception of raw image data versus information presented by gradient and saliency maps. The base image sequences represent original data from CARLA Town 1. We compare these to the gradient and saliency maps produced

Seq	m	Cosine	FID	SSIM	Confidence(%)
Level1	65	0.881	158.326	0.511	1.2
Level2	45	0.781	237.496	0.439	5.4
Level3	18	0.350	258.921	0.513	10.2
Level4	4	0.286	237.108	0.415	81.6

TABLE I

Quantitative study of cosine similarity trends over changes in **projected distance** in m meters. As projected distance decreases and the objects come closer, the classifier’s confidence of “collision” becomes significantly higher. As the collision confidence increases, the cosine similarity decreases since cosine similarity should correspond to confidence in the “safe” classification, which is noticeable here. On the contrary, FID and SSIM show inconsistent trends with respect to collision confidence.

by the same dataset, with samples taken from locations with same collision confidence. See comparison in Table II.

Seq	Technique	Cosine	FID	SSIM	Confidence(%)
1	Grad-CAM	0.635	512.73	0.0703	1.2
1	Vanilla	0.635	698.98	0.0576	1.2
2	Grad-CAM	0.568	493.94	0.0733	1.2
2	Vanilla	0.624	632.77	0.0557	1.2
3	Grad-CAM	0.632	403.62	0.0654	1.2
3	Vanilla	0.633	403.62	0.0654	1.2
$\tilde{\sigma}$	Both	0.0424	0.2296	0.1067	-
	Grad-CAM	0.0619	0.1240	0.0572	-
	Vanilla	0.0093	0.2679	0.0863	-

TABLE II

Quantitative study of cosine similarity metric in relation to **gradient visualization** data. We study two gradient techniques, Grad-CAM [23] and Vanilla backpropagation [24], across three different image sequences (involving scenario of the agent moving in with nearby vehicles) with equivalent classification confidence for “collision”. The cosine similarity shows consistent and constant results, i.e. a low standard deviation across different images with similar classification confidence. For FID and SSIM, we observe that normalized standard deviation $\tilde{\sigma}$ (i.e. σ/μ) is higher, and thus less reliable in measuring classifier confidence in learning.

These studies serve the purpose of validating cosine similarity as a suitable metric in analyzing its impact on decision making for driving, compared to two other well-known metrics. Next we use mean cosine similarity to measure the similarity between model perception of base image data and gradient/saliency maps for different scenarios using each one of the five spatio-temporal visual elements mentioned above. We observe these five global spatio-temporal features account for around a total contribution of 78% in the latent representations of the network, as shown in Table III.

C. Summary of Analysis

When using cosine similarity, smaller distances between vectors will yield a measurement closer to 1, while larger distances will be closer to -1. For projected distance, we observe that cosine similarity between feature vectors produces a consistent trend with classification confidence for the “collision” prediction, whereas FID and SSIM show inconsistent trends in capturing the same correlation. In level 1, where the change in the projected distance over an image

Seq	Spatio-Temporal features	Mean Significance (%)
1	Optical Flow	46
2	Rotational Component	28
3	Gradients	64
4	Moving cars and dynamic obstacles	16
μ	All Together	78

TABLE III

Quantitative analysis of the mean contribution in percentage of the global spatio-temporal features (including optical flow, agent’s orientation, spatial gradients across frames, and dynamic obstacles) in the networks decision making. We observe these features together account for around 78% contribution in the overall decision making of the network.

sequence is the least, we expect that a safe situation far away from a vehicle will remain safe since the projected distance barely changes over time. Likewise, in level 4, which features the largest change in projected distance over time, we observe that the cosine similarity between model-level representations drastically decreases, showing change in model decision making correlating to collision confidence.

Gradient results can be interpreted as the difference in learning perception between raw image data and gradient/saliency maps. For cosine similarity, we expect the similarity scores across sequences with similar collision confidences to be consistent. The bottom section of Table II shows the normalized standard deviation measurements across all sequences based on method and metric. For most cases, cosine similarity appears to be the most consistent metric in terms of retaining relevance to decision confidence.

V. EXPERIMENTS & RESULTS

Training Dataset. For model training, we collect image data from the CARLA driving simulator [1], version 0.9.5, with binary labels on “collision” data and “safe” data. The data is collected in 15-frame sequential stacks, which is necessary for LSTM training. Each image is of shape 420 by 280. Of a total dataset size of approximately 6,000 sequences, for both “collision” and “safe” scenarios. The training-validation split is 90-10. For testing, we reserve 2,000 images. We collected this data via the CARLA Python APIs, which allow us to selectively collect data leading up to a collision as well as general safe driving data.

A. Model Comparison.

The baseline model [2] is a similar transfer learning model that does not use LSTM nor take into account the hidden state representations of the source domain. The architecture is otherwise the same, except that only the resulting weights from the CNN would be used to initialize the target model in transfer learning. In this sense, we can measure the effect of transferring the LSTM hidden states and model weight initialization.

We compare the results of each model on test data from unseen environments or visual domains. The first test dataset represents an unseen driving environment within the same visual domain, CARLA [1] Town 2. The second and third test datasets represent environments from DeepDrive [25] and



Fig. 3. Representative Images of Training and Test Data (Left to Right): Training Data from CARLA Town 3 and CARLA Town 1; Test Data from Deep Drive, and Real-world YouTube Vehicle Collision Video.

Model	Test Dataset Accuracy (%)				
	CARLA Town2	DeepDrive	Audi	Honda	Youtube
Mean Cosine Similarity (to CARLA Town1)	0.77	0.697	0.623	0.591	0.55
Baseline Model [2]	71	65	63	60	59
Our CNN+LSTM with learned weights	88	80	75	73	76
Ours Overall	91	85	82	82	81
CNN+LSTM w/ txf weights Δ Improvement (%)	23.94	23.07	19.04	21.67	28.81
Ours Overall Δ Improvement (%)	29.58	30.77	30.15	36.6	37.29

TABLE IV

Comparison of accuracy performance (%) between the baseline model and our model across unseen environments and domains. Unseen test dataset include: 1) CARLA Town 2, which represents the same visual domain but a different environment, 2) DeepDrive [25], another popular driving simulator to represent a different virtual domain, and 3) real-world data collected from Audi [26] and YouTube collision videos. Both our model and the baseline are trained on Carla Town 1 dataset. We measure the semantic differences in each domain using cosine similarity; higher values indicate closer semantic relationships to the training dataset, and serve as a proxy indicator of transferability of learning across domains. We also compare our model with only transferred weights to our model overall, which involves transferred weights and saliency/gradient/edge maps. Between these two results, we observe that saliency, gradient, and edge maps can significantly improve test performance. **Overall, our model shows better generalization across environments** on which it was not trained by **29.58% up to 37.3%** improvement in accuracy over the baseline model [2].

Audi [26], while the last test dataset is real-world collision videos collected from YouTube. The binary classification task makes labeling of real-world data much more conveniently, where collision videos can be labeled “collision” while proper driving can be labeled “safe”. Examples of such images from training and test data can be found in Figure 3 to show the visual difference across domains. Table IV illustrates that our enhanced model outperformed the baseline in transfer learning on unseen domain data by up to 37.29%.

B. Observations and Discussion

We observe the following key findings in Table IV:

- The mean cosine similarity metric correlates linearly to the performance improvement in using our dynamics-aware transfer learning framework. Higher metric values correspond to higher similarity in the visual domains, thus benefiting less from the enhancement as expected given the base model should work well in similar domains. However, where the visual domains have significantly more disparity, such as in the case of ‘sim-to-real’, our enhanced transfer learning framework provides better generalization across domains (upto 37%).
- In visual domains with high similarity scores, the use of LSTM, along with the transfer of its hidden states (i.e. the model parameters or weights), can adequately capture the common spatio-temporal features in the model itself, thus sufficiently improve the transferability of the network training, as seen in ‘sim-to-sim’ case for

CARLA Town 1 and 2 (*or* Town 1 and DeepDrive).

- In visual domains with low similarity scores, the LSTM hidden states may not capture spatio-temporal features as well, the introduction of saliency, edges, and gradient maps together provide additional spatio-temporal information not already embedded in the network model, as in the ‘sim-to-real’ case between CARLA Town 1 and a collection of Youtube videos (*or* Audi driving data).

VI. CONCLUSION AND FUTURE WORK

In this work, we present three main contributions: 1) a CNN+LSTM model architecture for vision-based autonomous driving networks, 2) transfer of spatial and temporal features through transfer of LSTM hidden state embeddings and CNN weights, and 3) dynamics-aware spatio-temporal feature extraction to complement regular image data with saliency, gradient, and edge maps for training, where the model perception of visual elements using cosine similarity is used to select these features.

Contributions of this work could be extended to more complex learning tasks, such as multi-class classification, segmentation, or steering angle prediction. Another area for improvement is the streamlining of the data augmentation process. Gradient, saliency, and edge maps can be costly to produce in terms of time and resources; other alternatives or acceleration techniques could be explored.

REFERENCES

- [1] A. Dosovitskiy, G. Ros, F. Codevilla, A. Lopez, and V. Koltun, "CARLA: An open urban driving simulator," in *Proceedings of the 1st Annual Conference on Robot Learning*, 2017, pp. 1–16.
- [2] S. Akhauri, L. Zheng, and M. Lin, "Enhanced transfer learning for autonomous driving with systematic accident simulation," in *Proceedings of the IEEE/RSJ International Conference on Intelligent Robots and Systems (IROS)*, 2020.
- [3] M. Bojarski, D. D. Testa, D. Dworakowski, B. Firner, B. Flepp, P. Goyal, L. D. Jackel, M. Monfort, U. Muller, J. Zhang, X. Zhang, J. Zhao, and K. Zieba, "End to end learning for self-driving cars," *CoRR*, vol. abs/1604.07316, 2016. [Online]. Available: <http://arxiv.org/abs/1604.07316>
- [4] D. Bahdanau, K. Cho, and Y. Bengio, "Neural machine translation by jointly learning to align and translate," in *3rd International Conference on Learning Representations, ICLR 2015, San Diego, CA, USA, May 7-9, 2015, Conference Track Proceedings*, Y. Bengio and Y. LeCun, Eds., 2015. [Online]. Available: <http://arxiv.org/abs/1409.0473>
- [5] J. Ba, V. Mnih, and K. Kavukcuoglu, "Multiple object recognition with visual attention," in *3rd International Conference on Learning Representations, ICLR 2015, San Diego, CA, USA, May 7-9, 2015, Conference Track Proceedings*, Y. Bengio and Y. LeCun, Eds., 2015. [Online]. Available: <http://arxiv.org/abs/1412.7755>
- [6] S. Song, C. Lan, J. Xing, W. Zeng, and J. Liu, "Spatio-temporal attention-based lstm networks for 3d action recognition and detection," *IEEE Transactions on Image Processing*, vol. 27, no. 7, pp. 3459–3471, 2018.
- [7] J. Liu, G. Wang, L. Duan, K. Abdiyeva, and A. C. Kot, "Skeleton-based human action recognition with global context-aware attention lstm networks," *IEEE Transactions on Image Processing*, vol. 27, no. 4, pp. 1586–1599, 2018.
- [8] Z. Bai, B. Cai, W. ShangGuan, and L. Chai, "Deep learning based motion planning for autonomous vehicle using spatiotemporal lstm network," in *2018 Chinese Automation Congress (CAC)*, 2018, pp. 1610–1614.
- [9] Y. Zhang, P. David, and B. Gong, "Curriculum domain adaptation for semantic segmentation of urban scenes," in *Proceedings of the IEEE International Conference on Computer Vision (ICCV)*, Oct 2017.
- [10] W. Hong, Z. Wang, M. Yang, and J. Yuan, "Conditional generative adversarial network for structured domain adaptation," in *Proceedings of the IEEE Conference on Computer Vision and Pattern Recognition (CVPR)*, June 2018.
- [11] Z. Murez, S. Kolouri, D. Kriegman, R. Ramamoorthi, and K. Kim, "Image to image translation for domain adaptation," in *Proceedings of the IEEE Conference on Computer Vision and Pattern Recognition (CVPR)*, June 2018.
- [12] C. Liu, Y. Chen, L. Tai, H. Ye, M. Liu, and B. E. Shi, "A gaze model improves autonomous driving," in *Proceedings of the 11th ACM Symposium on Eye Tracking Research & Applications*, ser. ETRA '19. New York, NY, USA: Association for Computing Machinery, 2019. [Online]. Available: <https://doi.org/10.1145/3314111.3319846>
- [13] A. Pal, S. Mondal, and H. I. Christensen, "'looking at the right stuff' - guided semantic-gaze for autonomous driving," in *Proceedings of the IEEE/CVF Conference on Computer Vision and Pattern Recognition (CVPR)*, June 2020.
- [14] K. Weiss, T. M. Khoshgoftaar, and D. Wang, "A survey of transfer learning," *Journal of Big Data*, vol. 3, no. 1, p. 9, 2016. [Online]. Available: <https://doi.org/10.1186/s40537-016-0043-6>
- [15] M. L. Iuzzolino, M. E. Walker, and D. Szafr, "Virtual-to-real-world transfer learning for robots on wilderness trails," *CoRR*, vol. abs/1901.05599, 2019. [Online]. Available: <http://arxiv.org/abs/1901.05599>
- [16] Y. You, X. Pan, Z. Wang, and C. Lu, "Virtual to real reinforcement learning for autonomous driving," *CoRR*, vol. abs/1704.03952, 2017. [Online]. Available: <http://arxiv.org/abs/1704.03952>
- [17] A. Dosovitskiy and T. Brox, "Generating images with perceptual similarity metrics based on deep networks," in *Advances in neural information processing systems*, 2016, pp. 658–666.
- [18] A. Horé and D. Ziou, "Image quality metrics: Psnr vs. ssim," in *2010 20th International Conference on Pattern Recognition*, 2010, pp. 2366–2369.
- [19] S. Albitar, S. Fournier, and B. Espinasse, "An effective tf/idf-based text-to-text semantic similarity measure for text classification," in *Web Information Systems Engineering – WISE 2014*, B. Benatallah, A. Bestavros, Y. Manolopoulos, A. Vakali, and Y. Zhang, Eds. Cham: Springer International Publishing, 2014, pp. 105–114.
- [20] M. Heusel, H. Ramsauer, T. Unterthiner, B. Nessler, and S. Hochreiter, "Gans trained by a two time-scale update rule converge to a local nash equilibrium," in *Proceedings of the 31st International Conference on Neural Information Processing Systems*, ser. NIPS'17. Red Hook, NY, USA: Curran Associates Inc., 2017, p. 6629–6640.
- [21] M. Seitzer, "pytorch-fid: FID Score for PyTorch," <https://github.com/mseitzer/pytorch-fid>, August 2020, version 0.1.1.
- [22] Zhou Wang, A. C. Bovik, H. R. Sheikh, and E. P. Simoncelli, "Image quality assessment: from error visibility to structural similarity," *IEEE Transactions on Image Processing*, vol. 13, no. 4, pp. 600–612, 2004.
- [23] R. R. Selvaraju, M. Cogswell, A. Das, R. Vedantam, D. Parikh, and D. Batra, "Grad-cam: Visual explanations from deep networks via gradient-based localization," in *2017 IEEE International Conference on Computer Vision (ICCV)*, 2017, pp. 618–626.
- [24] K. Simonyan, A. Vedaldi, and A. Zisserman, "Deep inside convolutional networks: Visualising image classification models and saliency maps," in *Workshop at International Conference on Learning Representations*, 2014.
- [25] Voyage, "Deepdrive." [Online]. Available: <https://deepdrive.voyage.auto/>
- [26] J. Geyer, Y. Kassahun, M. Mahmudi, X. Ricou, R. Durgesh, A. S. Chung, L. Hauswald, V. H. Pham, M. Mühlegg, S. Dorn, T. Fernandez, M. Jänicke, S. Mirashi, C. Savani, M. Sturm, O. Vorobiov, M. Oelker, S. Garreis, and P. Schuberth, "A2D2: Audi Autonomous Driving Dataset," 2020. [Online]. Available: <https://www.a2d2.audi>

Seq	Scenario for spatio-temporal features measurement	Mean Cosine
1	Agent moving with nearby vehicles	0.7983
2	Agent moving on empty roads	0.8887
3	Agent turning	0.732
4	Agent stationary with dynamic obstacles around	0.712
μ	All	0.7827

TABLE V

A scenario-based case study on the role of spatio-temporal features: It includes agent’s orientation, optical flow of the edge information across frames, dynamic obstacles and moving vehicles using the approach described for the ablation study. We also perform a study on the combination of the role of the four global spatio-temporal features including optical flows, rotational components, gradient flows and dynamic obstacles. We observe that these features together account for about 78%, while other spatial features in the background contributing 22%, towards the agent’s decision making.

Seq	Agent orientation(wrt the lane center)	Mean Cosine
1	70-80	0.3454
2	50-60	0.32
3	30-40	0.2908
4	5-20	0.159
μ	All	0.277

TABLE VI

Quantitative analysis on impact of the agent’s orientation across frames in the latent representations using cosine similarity metric. We observe that the agent’s change in orientation as a spatio-temporal feature accounts for 28% contribution in the hidden state representations of the trained model.

Seq	Scenario for Optical Flow temporal feature measurement	Mean Cosine
1	Agent moving with nearby vehicles	0.48
2	Agent moving on empty roads	0.40
3	Agent turning	0.54
4	Agent stationary with dynamic obstacles around	0.42
μ	All	0.46

TABLE VII

Quantitative analysis on impact of the optical flows across frames in the network latent representations using cosine similarity metric. We observe that optical flows as a spatio-temporal feature accounts for around 46% contribution in the hidden state representations of the trained network.

Seq	Scenario for Dynamic obstacles feature measurement	Mean Cosine
1	Agent moving with nearby vehicles	0.18
2	Agent moving on empty roads	0.13
3	Agent turning	0.14
4	Agent stationary with dynamic obstacles around	0.18
μ	All	0.157

TABLE VIII

Quantitative analysis on impact of dynamic obstacles across frames in the network latent representations using cosine similarity metric. We observe that dynamic obstacles as a spatio-temporal feature accounts for around 16% contribution in the hidden states of the trained model.